Extension of the GMMV-Based Linear Method to Quantitative Inverse Scattering

Shilong Sun, Bert Jan Kooij, and Alexander G. Yarovoy, *Fellow, IEEE*

***Abstract*—The linear shape reconstruction method based on the generalized multiple measurement vectors model is a newly proposed approach that is able to effectively retrieve the morphological information of dielectric/metallic scatterers with competitive imaging resolution. In this letter, we have extended this approach to quantitative inversion, with which a coarse estimation of the dielectric parameters can be obtained in an efficient way. The inversion of the transverse magnetic polarized Fresnel datasets from the year 2005 demonstrates applicability of the proposed method to real-life applications.**

***Index Terms*—Generalized multiple measurement vectors (GMMV), linear shape reconstruction method, quantitative inverse scattering, transverse magnetic (TM).**

I. Introduction

INVERSE electromagnetic (EM) scattering is a procedure of recovering the morphological information or the dielectric parameters of unknown objects using the probed scattered fields. Such an inverse problem is ill-posed and nonlinear due to the compactness and nonlinearity of the scattering operator [1], and therefore, seeking the solution is full of challenges.

To deal with the nonlinearity, Born approximation has been considered in methods, such as the (Distorted) Born iterative methods (BIM and DBIM) [2], [3] and the contrast source extended Born method [4]. Another group of methods are the nonlinear iterative methods, among which are the modified gradient method [5], the contrast source inversion (CSI) method [6], the cross-correlated CSI method [7], and the subspace optimization method [8]. All these methods are local iterative optimization methods and are, therefore, prone to the occurrence of false solutions [9]. Hybrid inversion methods [10], [11] have been proposed to first determine the support of the scatterers by qualitative inversion methods, and then exploit such *a priori* information for quantitative inversion. Multiscaling methods [12], [13] propose to use different resolution accuracies depending on the homogeneity of the media for reducing the occurrence of the local minima. In cases where the dimension of the solution space is not so huge, global optimization techniques [14]–[16] are good candidates to search for the global optimal solution.

Manuscript received August 31, 2017; revised November 6, 2017; accepted November 20, 2017. Date of publication November 22, 2017; date of current version January 10, 2018. *(Corresponding author: Shilong Sun).*

The authors are with the Delft University of Technology, Delft 2628, The Netherlands (e-mail: ShilongSun@126.com; B.J.Kooij@tudelft.nl; A.Yarovoy@tudelft.nl).

Digital Object Identifier 10.1109/LAWP.2017.2776526

Apart from the approaches of linearizing the inverse scattering problem based on the approximate scattering models, the linear sampling method (LSM) [17], [18] enables the retrieval of the morphological features of the scatterers by solving a linear system of equations. A quantitative inversion of LSM based on "virtual experiments" was further proposed in [19]–[21]. Recently, a linear shape reconstruction method based on the multiple measurement vectors (MMV) model was first proposed in [22] for solving the PEC inverse scattering problem, and was later extended to the inversion of 3-D dielectric/metallic scatterers in [23]. A multifrequency version of this method was proposed in [24] based on the generalized MMV (GMMV) model, which turns out to be of higher resolving ability than LSM [24]. As a major difference of the GMMV method compared to compressive sensing methods [25], [26], an estimated solution of the contrast sources regularized by the sum-of-norm constraint is demonstrated to be sufficient for recovering the spatial profile of the nonsparse targets.

In this letter, we propose an extended version of the GMMV-based linear method for solving the quantitative inverse scattering problem. The contrast sources are first reconstructed by the GMMV-based linear method, then the contrast can be finally estimated as the least-square solution to the multifrequency state equations. Although the estimation accuracy is not high, this approach turns out to be efficient and robust in the inversion of experimental data. The proposed method is introduced in Section II and applied to process the transverse magnetic (TM) polarized Fresnel datasets [27] in Section III.

II. Quantitative Inversion by GMMV-Based Linear Method

A. Formulation of the Inverse Scattering Problem

For the sake of simplicity, we consider the 2-D TM-polarized EM scattering problem, for which the electric field is a scalar. Assume the background is known to a reasonable accuracy, and the permeability of the background and unknown objects is a constant μ_0. The objects are illuminated by sources from different angles denoted by the subscript $p \in \{1, 2, 3, \ldots, P\}$, and the scattered fields are measured with receivers at different positions denoted by the subscript $q \in \{1, 2, 3, \ldots, Q\}$, which yields the data equations [24]

$$\boldsymbol{y}_{p,i} = \boldsymbol{\Phi}_{p,i} \boldsymbol{j}^{ic}_{p,i}, \quad p = 1, 2, \ldots, P,\ i = 1, 2, \ldots, I \tag{1}$$

where $\boldsymbol{\Phi}_{p,i} = \mathcal{M}^{\mathcal{S}}_{p} \boldsymbol{A}_i^{-1} \omega_i \in \mathbb{C}^{Q \times N}$ is the sensing matrix for the measurement $\boldsymbol{y}_{p,i}$, and $\boldsymbol{j}^{ic}_{p,i} = \omega_i \boldsymbol{j}_{p,i}$ is the normalized

contrast source that is proportional to the physical induced current $\mathbf{i}\omega_i\mu_0\boldsymbol{j}_{p,i}$. Here, ω_i is the ith angular frequency; $\mathbf{i}$ represents the unit of the imaginary part of complex numbers; $\boldsymbol{j}_{p,i} = \boldsymbol{\chi}_i \boldsymbol{e}^{\text{tot}}_{p,i}$ is the contrast source; $\boldsymbol{\chi}_i = \Delta\varepsilon - \mathbf{i}\Delta\sigma/\omega_i$ is the contrast with $\Delta\varepsilon$ and $\Delta\sigma$ representing the contrast permittivity and contrast conductivity, respectively; $\boldsymbol{e}^{\text{tot}}_{p,i}$ represents the total field; $\boldsymbol{A}_i \in \mathbb{C}^{N\times N}$ is the stiffness matrix in finite-difference frequency-domain (FDFD) scheme at the ith frequency, which is highly sparse; $\mathcal{M}_p^{\mathcal{S}}$ is a measurement matrix selecting the values of the pth scattered field at the positions of Q receivers. The time factor considered in this letter is $\exp(\mathbf{i}\omega_i t)$.

B. GMMV-Based Linear Method

In the GMMV-based linear method [24], the contrast sources are estimated by iteratively solving a sum-of-norm optimization problem

$$\min \quad \|\boldsymbol{J}\|_{1,2} \quad \text{s. t.} \quad \|\boldsymbol{\Phi}\cdot\boldsymbol{J} - \boldsymbol{Y}\|_F \le \tilde{\sigma} \tag{2}$$

where $\|\boldsymbol{J}\|_{1,2} := \sum_{n=1}^{N} \left\|\boldsymbol{J}[n,:]^T\right\|_2$, in which $\boldsymbol{J}[n,:]$ denotes the nth row of $\boldsymbol{J}$ and $(\cdot)^T$ is the transpose operator; $\boldsymbol{Y} = [\boldsymbol{y}_{1,1}\ \boldsymbol{y}_{2,1}\ \cdots\ \boldsymbol{y}_{P,1}\ \boldsymbol{y}_{1,2}\ \cdots\ \boldsymbol{y}_{P,I}] \in \mathbb{C}^{Q\times PI}$ is the multifrequency measurement data matrix; $\boldsymbol{J} = [\boldsymbol{j}^{ic}_{1,1}\ \boldsymbol{j}^{ic}_{2,1}\ \cdots\ \boldsymbol{j}^{ic}_{P,1}\ \boldsymbol{j}^{ic}_{1,2}\ \cdots\ \boldsymbol{j}^{ic}_{P,I}] \in \mathbb{C}^{N\times PI}$ is the normalized contrast sources matrix, of which the columns are the multiple vectors to be solved; $\boldsymbol{\Phi}\cdot\boldsymbol{J} := [\boldsymbol{\Phi}_{1,1}\boldsymbol{j}^{ic}_{1,1}\ \boldsymbol{\Phi}_{2,1}\boldsymbol{j}^{ic}_{2,1}\ \ldots\ \boldsymbol{\Phi}_{P,I}\boldsymbol{j}^{ic}_{P,I}]$; $\|\cdot\|_F$ is the Frobenius norm; and $\tilde{\sigma}$ represents the noise residual. As an equivalent problem of (2), the GMMV$_{\text{TM}}$ LS$_\tau$ problem is reformulated as

$$(\text{GMMV}_{\text{TM}}\ \text{LS}_\tau)\ \min\ \|\boldsymbol{\Phi}\cdot\boldsymbol{J} - \boldsymbol{Y}\|_F\ \text{ s.t. }\ \|\boldsymbol{J}\|_{1,2} \le \tau \tag{3}$$

and the Pareto curve for the GMMV model is defined as

$$\phi_{\text{GMMV}_{\text{TM}}}(\tau) = \|\boldsymbol{\Phi}\cdot\boldsymbol{J}_\tau - \boldsymbol{Y}\|_F \tag{4}$$

where $\boldsymbol{J}_\tau$ is the optimal solution to the LS$_\tau$ problem (3). According to [28, Th. 2.2] and [29, Ch. 5], $\phi_{\text{GMMV}_{\text{TM}}}(\tau)$ is continuously differentiable and

$$\phi'_{\text{GMMV}_{\text{TM}}}(\tau_h) = -\frac{\left\|\boldsymbol{\Phi}^H\cdot(\boldsymbol{\Phi}\cdot\boldsymbol{J}_{\tau_h} - \boldsymbol{Y})\right\|_{\infty,2}}{\|\boldsymbol{\Phi}\cdot\boldsymbol{J}_{\tau_h} - \boldsymbol{Y}\|_F} \tag{5}$$

where $\|\cdot\|_{\infty,2}$ is the dual norm of $\|\cdot\|_{1,2}$ [28, Corollary 6.2]. Similarly, the root of the nonlinear equation $\phi_{\text{MMV}_{\text{TM}}}(\tau) = \tilde{\sigma}$ can also be reached by Newton iterations

$$\tau_{h+1} = \tau_h + \frac{\tilde{\sigma} - \phi_{\text{GMMV}_{\text{TM}}}(\tau_h)}{\phi'_{\text{GMMV}_{\text{TM}}}(\tau_h)}. \tag{6}$$

The GMMV$_{\text{TM}}$ LS$_\tau$ problem can be solved using a spectral projected gradient method that is proposed based on convex optimization theory [30]–[32], which is similar with [33, Algorithm 1], except that the projection operator is replaced by an orthogonal projection onto $\|\cdot\|_{1,2}$ balls

$$\mathcal{P}_\tau[\boldsymbol{J}] := \left\{\arg\min_{\boldsymbol{X}}\ \|\boldsymbol{J} - \boldsymbol{X}\|_F\ \text{ s.t. }\ \|\boldsymbol{X}\|_{1,2} \le \tau\right\}. \tag{7}$$

We refer to [28, Th. 6.3] for the implementation of the projection operator. To circumvent the estimation of the noise level, cross-correlation (CV) technique is exploited to terminate the iteration. Since the regularized solution corresponds to the least sum-of-norm, the nonmeasurable equivalent contrast sources tend to be ignored.

C. Estimating the Contrast

Once the contrast sources are obtained, we calculate the scattered fields by $\boldsymbol{e}^{\text{sct}}_{p,i} = \boldsymbol{A}_i^{-1}\omega_i^2\boldsymbol{j}_{p,i}$ and the total fields by $\boldsymbol{e}^{\text{tot}}_{p,i} = \boldsymbol{e}^{\text{inc}}_{p,i} + \boldsymbol{e}^{\text{sct}}_{p,i}$. It is worth noting that, since we are only interested in the fields of the inversion domain, the stiffness matrix $\boldsymbol{A}_i$ can be reconstructed such that it only covers the inversion domain and the dimension of problem can be reduced. This is of great importance especially for the large-scale inverse scattering problems. Assuming that the dielectric parameters of the scatterer are frequency-independent, the contrast corresponding the first frequency—$\boldsymbol{\chi}_1$—can be obtained by the least-square solution of the multifrequency state equations $\boldsymbol{j}_{p,i} = \boldsymbol{\chi}_i \odot \boldsymbol{e}^{\text{tot}}_{p,i}$, which is given by

$$\begin{aligned}\boldsymbol{\chi}_1 = {} & \Re\left\{\sum_{i=1}^{I}\sum_{p=1}^{P}\boldsymbol{j}_{p,i}\odot\overline{\boldsymbol{e}^{\text{tot}}_{p,i}}\right\}\oslash\left(\sum_{i=1}^{I}\sum_{p=1}^{P}\boldsymbol{e}^{\text{tot}}_{p,i}\odot\overline{\boldsymbol{e}^{\text{tot}}_{p,i}}\right)\\ & +\mathbf{i}\Im\left\{\sum_{i=1}^{I}\frac{\omega_1}{\omega_i}\sum_{p=1}^{P}\boldsymbol{j}_{p,i}\odot\overline{\boldsymbol{e}^{\text{tot}}_{p,i}}\right\}\oslash\left(\sum_{i=1}^{I}\frac{\omega_1^2}{\omega_i^2}\sum_{p=1}^{P}\boldsymbol{e}^{\text{tot}}_{p,i}\odot\overline{\boldsymbol{e}^{\text{tot}}_{p,i}}\right)\end{aligned} \tag{8}$$

where $\odot$ and $\oslash$ represent the elementwise multiplication and the elementwise division, respectively; $\overline{(\cdot)}$ represents the complex conjugate of a number or a vector; $\Re\{\cdot\}$ and $\Im\{\cdot\}$ represent the real part and imaginary part of a number or a vector, respectively. Considering the relation $\boldsymbol{\chi} = \boldsymbol{\epsilon} - \boldsymbol{\epsilon}_b$, where $\boldsymbol{\epsilon}$ and $\boldsymbol{\epsilon}_b$ are the complex permittivity of the test domain and the background, and noting the fact that $\Re\{\boldsymbol{\epsilon}\} \succeq \mathbf{1}$, $\Im\{\boldsymbol{\epsilon}\} \preceq \mathbf{0}$, we can simply obtain

$$\Re\{\boldsymbol{\chi}\} \succeq \mathbf{1} - \Re\{\boldsymbol{\epsilon}_b\} \quad \Im\{\boldsymbol{\chi}\} \preceq -\Im\{\boldsymbol{\epsilon}_b\} \tag{9}$$

where $\succeq$ and $\preceq$ represent the componentwise inequality of two vectors. Therefore, the real part and the imaginary part of the elements that do not satisfy (9) are forced to $1 - \Re\{\boldsymbol{\epsilon}_{b,k}\}$ and $-\Im\{\boldsymbol{\epsilon}_{b,k}\}$, respectively.

III. Inversion With Experimental Data

A. Configuration

To validate the proposed GMMV-based linear inversion method, we applied it to the TM-polarized experimental datasets: *FoamDielIntTM* and *FoamMetExtTM*, provided by the Remote Sensing and Microwave Experiments Team at the Institut Fresnel, France, 2005 [27]. The measurement configuration is shown in Fig. 1(a), in which the diamond represents the transmitter, the 4×9 red ones are the CV measurements, and the black dots are the reconstruction measurements. To guarantee the accuracy of the FDFD scheme, the inversion domain is discretized with a grid size Δ^2 satisfying $\Delta \le \min\{\lambda_i\}/15$. We restrict the inversion domain to 150 $\times$ 150 mm^2 centered at

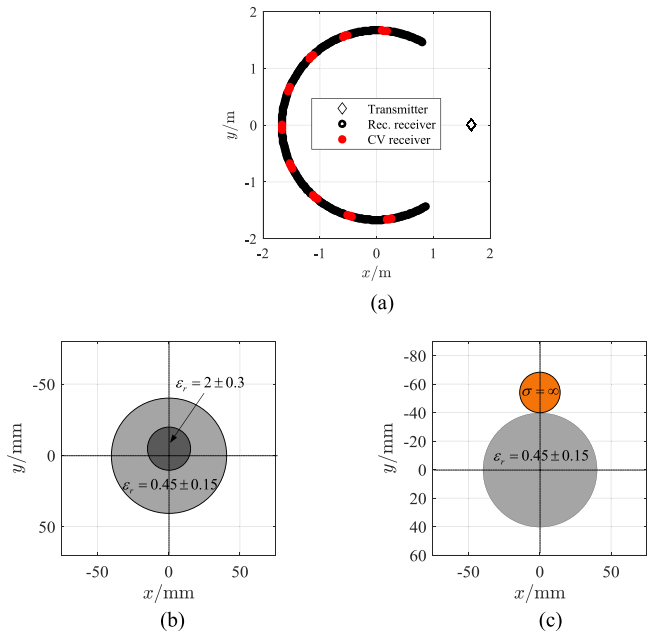

Fig. 1. Measurement configuration of the experimental data. (a) cross section of the true objects, (b) *FoamDielIntTM*, (c) *FoamMetExtTM*.

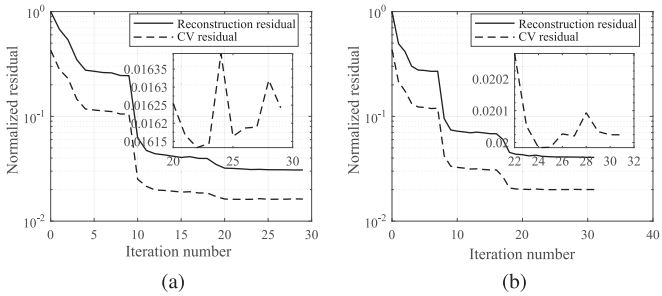

Fig. 2. Reconstruction residual curve and CV residual curve in the experimental examples. (a) *FoamDielIntTM*. (b) *FoamMetExtTM*.

the centroids of the scatterers, respectively, and the inversion domain is discretized with the same grid size of $1.0 \times 1.0\ \text{mm}^2$.

B. Inverted Results

1) FoamDielIntTM: The program is implemented with MATLAB codes. We ran the codes on a desktop with one Intel Core i5-3470 CPU at 3.20 GHz, and parallel computing was not used. Let us first consider the dataset *FoamDielIntTM*, whose configuration is shown in Fig. 1(b). Multifrequency data at 2, 3, and 4 GHz are processed by the proposed method. Fig. 2(a) gives the residual curves, and the optimal solution corresponds to the 22nd iteration. In solving one (LS_τ) problem [24], the decreasing rate of the residual curve is fast for the first few iterations and gets slower and slower as the algorithm converges. Since more than one (LS_τ) problem is solved, the residual curve presents a stair-like shape. Fig. 3(a) and (b) shows the permittivity and conductivity of the estimated contrast, respectively. Artifacts of maximum value 0.15 mS/m (corresponding to $|\Im\{\chi_1\}| = |-0.0014| \ll |\Re\{\chi_1\}|$ and, therefore, can be neglected) occur in Fig. 3(b). The total running time is 4.8 s, which only allows four iterations for the multifrequency version of

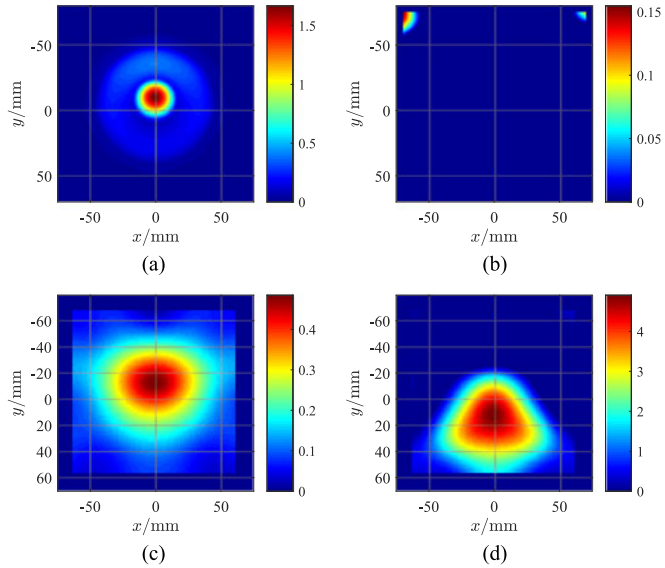

Fig. 3. Inverted results by processing *FoamDielIntTM* at 2, 3, and 4 GHz. (a) Relative permittivity and (b) conductivity of contrast obtained by the proposed method; (c) relative permittivity and (d) conductivity of contrast obtained by MR-CSI with four iterations. Unit of conductivity is mS/m.

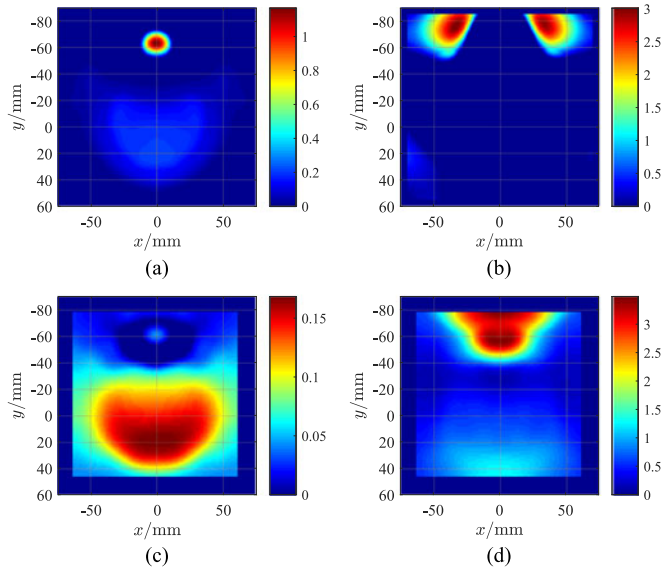

Fig. 4. Inverted result by processing *FoamMetExtTM* at 2, 3, and 10 GHz. (a) Relative permittivity and (b) conductivity of contrast obtained by the proposed method; (c) relative permittivity and (d) conductivity of contrast obtained by MR-CSI with four iterations. Unit of conductivity is mS/m.

the multiplicative regularized CSI method (MR-CSI) [34] [see Fig. 3(c) and (d) for the corresponding inverted results]. Define the reconstruction error by $\text{err} = \|\chi - \hat{\chi}\|/\|\chi\|$, we have $\text{err}_{\text{GMMV}} = 0.70 < \text{err}_{\text{MR-CSI}} = 0.76$.

2) FoamMetExtTM: In contrast to the previous experiment, the *FoamMetExtTM* dataset is obtained using 18 transmitters, while other settings are kept the same. Fig. 1(c) shows the configuration. We process this dataset at nine frequencies of 2–10 GHz. Fig. 2(b) gives the residual curves and the optimal solution corresponds to the 24th iteration. Fig. 4(a) and

(b) shows the relative permittivity and conductivity of the estimated contrast, respectively. The total running time is 30 s, which only allows four iterations for the multifrequency version of MR-CSI [see Fig. 4(c) and (d) for the corresponding inverted results]. Artifacts of maximum value 3 mS/m (corresponding to $|\Im\{\chi_1\}| = |-0.027| \ll |\Re\{\chi_1\}|$ and, therefore, can be neglected) occur in Fig. 4(b). The reconstruction error does not make any sense and is not given in this example because a metallic tube is considered whose conductivity is infinity.

Considering both the inversion accuracy and the computational complexity ($\mathcal{O}(n^2)$ for the GMMV method and $\mathcal{O}(n^k)$ with $k > 2$ for MR-CSI), the proposed method is a good candidate for an efficient estimation of the contrast, especially in 3-D domain. It is also worth comparing the computational complexity of the proposed method with the linear method based on LSM and "virtual experiments." As LSM solves $\boldsymbol{G}$ from $\boldsymbol{\Phi G} = \boldsymbol{Y}$ and MMV solves $\boldsymbol{J}$ from $\boldsymbol{YJ} = \boldsymbol{\Phi}$, the two models are equivalent to some extent. Higher resolving ability of MMV comes from the exploitation of sum-of-norm regularized constraint. The "virtual experiments" framework needs to solve SVD of a matrix $\boldsymbol{L} \in \mathbb{C}^{(P\times M\times I)\times N}$. In 3-D problems, $\boldsymbol{L}$ could be a huge matrix and solving the SVD of huge matrix is time-consuming.

IV. Conclusion

In this letter, we have extended the linear shape reconstruction method based on the GMMV model to solve quantitative inverse scattering problems. The inverted results by processing the experimental Fresnel datasets demonstrate the validity. In many applications, it is of interest if computational efficiency has higher priority, while the requirement of the estimation accuracy is not strict. In addition, it also provides a good initial estimate for the iterative inversion methods.

References

[1] D. Colton and R. Kress, *Inverse Acoustic and Electromagnetic Scattering Theory*, vol. 93. New York, NY, USA: Springer, 2013.

[2] Y. Wang and W. C. Chew, "An iterative solution of the two-dimensional electromagnetic inverse scattering problem," *Int. J. Imag. Syst. Technol.*, vol. 1, no. 1, pp. 100–108, 1989.

[3] W. C. Chew and Y.-M. Wang, "Reconstruction of two-dimensional permittivity distribution using the distorted Born iterative method," *IEEE Trans. Med. Imag.*, vol. 9, no. 2, pp. 218–225, Jun. 1990.

[4] T. Isernia, L. Crocco, and M. D'Urso, "New tools and series for forward and inverse scattering problems in lossy media," *IEEE Geosci. Remote Sens. Lett.*, vol. 1, no. 4, pp. 327–331, Oct. 2004.

[5] R. Kleinman and P. Van den Berg, "A modified gradient method for two-dimensional problems in tomography," *J. Comput. Appl. Math.*, vol. 42, no. 1, pp. 17–35, 1992.

[6] P. M. Van Den Berg and R. E. Kleinman, "A contrast source inversion method," *Inverse Probl.*, vol. 13, no. 6, pp. 1607–1620, 1997.

[7] S. Sun, B. J. Kooij, T. Jin, and A. G. Yarovoy, "Cross-correlated contrast source inversion," *IEEE Trans. Antennas Propag.*, vol. 65, no. 5, pp. 2592–2603, May 2017.

[8] X. Chen, "Subspace-based optimization method for solving inverse-scattering problems," *IEEE Trans. Geosci. Remote Sens.*, vol. 48, no. 1, pp. 42–49, Jan. 2010.

[9] T. Isernia, V. Pascazio, and R. Pierri, "On the local minima in a tomographic imaging technique," *IEEE Trans. Geosci. Remote Sens.*, vol. 39, no. 7, pp. 1596–1607, Jul. 2001.

[10] I. Catapano, L. Crocco, M. D'Urso, and T. Isernia, "On the effect of support estimation and of a new model in 2-D inverse scattering problems," *IEEE Trans. Antennas Propag.*, vol. 55, no. 6, pp. 1895–1899, Jun. 2007.

[11] M. Brignone, G. Bozza, A. Randazzo, M. Piana, and M. Pastorino, "A hybrid approach to 3D microwave imaging by using linear sampling and ACO," *IEEE Trans. Antennas Propag.*, vol. 56, no. 10, pp. 3224–3232, Oct. 2008.

[12] P. Chiappinelli, L. Crocco, T. Isernia, and V. Pascazio, "Multiresolution techniques in microwave tomography and subsurface sensing," in *Proc. IEEE Int. Geosci. Remote Sens. Symp.*, Jul. 1999, vol. 5, pp. 2516–2518.

[13] S. Caorsi, M. Donelli, and A. Massa, "Detection, location, and imaging of multiple scatterers by means of the iterative multiscaling method," *IEEE Trans. Microw. Theory Techn.*, vol. 52, no. 4, pp. 1217–1228, Apr. 2004.

[14] S. Caorsi, A. Massa, and M. Pastorino, "A crack identification microwave procedure based on a genetic algorithm for nondestructive testing," *IEEE Trans. Antennas Propag.*, vol. 49, no. 12, pp. 1812–1820, Dec. 2001.

[15] P. Rocca, M. Benedetti, M. Donelli, D. Franceschini, and A. Massa, "Evolutionary optimization as applied to inverse scattering problems," *Inverse Probl.*, vol. 25, no. 12, 2009, Art. no. 123003.

[16] M. Salucci, L. Poli, N. Anselmi, and A. Massa, "Multifrequency particle swarm optimization for enhanced multiresolution GPR microwave imaging," *IEEE Trans. Geosci. Remote Sens.*, vol. 55, no. 3, pp. 1305–1317, Mar. 2017.

[17] D. Colton and A. Kirsch, "A simple method for solving inverse scattering problems in the resonance region," *Inverse Probl.*, vol. 12, no. 4, pp. 383–393, 1996.

[18] L. Crocco, L. Di Donato, I. Catapano, and T. Isernia, "An improved simple method for imaging the shape of complex targets," *IEEE Trans. Antennas Propag.*, vol. 61, no. 2, pp. 843–851, Feb. 2013.

[19] L. Crocco, I. Catapano, L. Di Donato, and T. Isernia, "The linear sampling method as a way to quantitative inverse scattering," *IEEE Trans. Antennas Propag.*, vol. 60, no. 4, pp. 1844–1853, Apr. 2012.

[20] L. Di Donato, R. Palmeri, G. Sorbello, T. Isernia, and L. Crocco, "A new linear distorted-wave inversion method for microwave imaging via virtual experiments," *IEEE Trans. Microw. Theory Techn.*, vol. 64, no. 8, pp. 2478–2488, Aug. 2016.

[21] R. Palmeri, M. T. Bevacqua, L. Crocco, T. Isernia, and L. Di Donato, "Microwave imaging via distorted iterated virtual experiments," *IEEE Trans. Antennas Propag.*, vol. 65, no. 2, pp. 829–838, Feb. 2017.

[22] S. Sun, B. J. Kooij, and A. G. Yarovoy, "Solving the PEC inverse scattering problem with a linear model," in *Proc. URSI Int. Symp. Electromagn. Theory*, Aug. 2016, pp. 144–147.

[23] S. Sun, B. J. Kooij, and A. G. Yarovoy, "Linearized 3-D electromagnetic contrast source inversion and its applications to half-space configurations," *IEEE Trans. Geosci. Remote Sens.*, vol. 55, no. 6, pp. 3475–3487, Jun. 2017.

[24] S. Sun, B. J. Kooij, A. Yarovoy, and T. Jin, "A linear method for shape reconstruction based on the generalized multiple measurement vectors model," *IEEE Trans. Antennas Propag.*, to be published.

[25] L. Poli, G. Oliveri, F. Viani, and A. Massa, "MT–BCS-based microwave imaging approach through minimum-norm current expansion," *IEEE Trans. Antennas Propag.*, vol. 61, no. 9, pp. 4722–4732, Sep. 2013.

[26] M. Bevacqua and T. Isernia, "Shape reconstruction via equivalence principles, constrained inverse source problems and sparsity promotion," *Prog. Electromagn. Res.*, vol. 158, pp. 37–48, Feb. 2017.

[27] J.-M. Geffrin, P. Sabouroux, and C. Eyraud, "Free space experimental scattering database continuation: experimental set-up and measurement precision," *Inverse Probl.*, vol. 21, no. 6, pp. S117–S130, 2005.

[28] E. Van den Berg and M. P. Friedlander, "Sparse optimization with least-squares constraints," *SIAM J. Optim.*, vol. 21, no. 4, pp. 1201–1229, 2011.

[29] E. van den Berg, "Convex optimization for generalized sparse recovery," Ph.D. dissertation, Univ. British Columbia, Vancouver, BC, Canada, 2009.

[30] E. G. Birgin, J. M. Martínez, and M. Raydan, "Nonmonotone spectral projected gradient methods on convex sets," *SIAM J. Optim.*, vol. 10, no. 4, pp. 1196–1211, 2000.

[31] E. G. Birgin, J. M. Martínez, and M. Raydan, "Inexact spectral projected gradient methods on convex sets," *IMA J. Numer. Anal.*, vol. 23, no. 4, pp. 539–559, 2003.

[32] Y.-H. Dai and R. Fletcher, "Projected Barzilai–Borwein methods for large-scale box-constrained quadratic programming," *Numer. Math.*, vol. 100, no. 1, pp. 21–47, 2005.

[33] E. van den Berg and M. P. Friedlander, "Probing the Pareto frontier for basis pursuit solutions," *SIAM J. Sci. Comput.*, vol. 31, no. 2, pp. 890–912, 2008.

[34] R. F. Bloemenkamp, A. Abubakar, and P. M. Van Den Berg, "Inversion of experimental multi-frequency data using the contrast source inversion method," *Inverse Probl.*, vol. 17, no. 6, pp. 1611–1622, 2001.